The 8th European Congress on Computational Methods in Applied Sciences and Engineering
ECCOMAS Congress 2022
5–9 June 2022, Oslo, Norway

NUMERICAL SIMULATION OF THE MICRO-EXTRUSION PROCESS OF PRINTABLE BIOMATERIALS

Ahmad Amani[1], Deniz Kizildag[1], Jesús Castro[1], Laura del-Mazo-Barbara[2], Marta Pegueroles[2], Maria-Pau Ginebra[2]

[1] Heat and Mass Transfer Technological Center, Technical University of Catalonia, Carrer de Colom 11, 08222 Terrassa (Barcelona), Spain; www.cttc.upc.edu

[2] Biomaterials, Biomechanics and Tissue Engineering Group, Department of Materials Science and Engineering, Universitat Politècnica de Catalunya (UPC), Av. Eduard Maristany 16, 08019, Barcelona, Spain
{ahmad.amani, deniz.kizildag, jesus.castro, laURa.del.mazo, marta.pegueroles, maria.pau.ginebra}@upc.edu

Key words: Direct Numerical Simulation (DNS), extrusion process, 3D printers

Abstract. This work aims to gain a better understanding of how the rheological properties of printable materials affect their processability, as well as the quality of the final product, which at the end can lead to reducing time and costs of the process and increase product development.

As the first step, the proper rheological non-Newtonian models are extracted from experimental studies. Later, three-dimensional numerical simulation of extrusion process is performed in the context of Direct Numerical Simulation (DNS) of governing equations, where the whole physics of fluid motion is taken into account. A finite-volume fractional step approach is used to solve the Navier-Stocks equations on collocated arbitrary meshes. Geometrical volume-of-fluid (GVOF) interface capturing approach is used to resolve the topological changes of the moving interface. The governing equations are solved using High-Performance Computing (HPC) parallel approaches.

Besides the contribution of this work to the advancement of numerical techniques applied to multiphase complex flows, obtained results will shed light on the nature of non-Newtonian extrusion process with vast applications in the 3D printer industrial sectors.

1 INTRODUCTION

3D printing has opened up new perspectives in the field of personalised medicine, with the possibility of manufacturing patient-specific implants or even bioprinting cells through microextrusion processes. Different types of inks have been developed for this purpose, with a wide spectrum of rheological properties, ranging from very thick ceramic pastes to very soft hydrogels. The knowledge and modelling of how rheological properties affect printability is an indispensable tool to design inks with better performance and to improve printing processes. The current study presents numerical simulations of the micro-extrusion process of printable biomaterials, focusing more specifically on ceramic inks that consist of a thick suspension of ceramic particles in a polymeric binder. This type of inks is used to fabricate

customized implants for the repair and regeneration of bone defects. The rheological properties of these inks, extracted from experimental data, are used to establish the rheological non-Newtonian models that are subsequently fed to the numerical simulations.

The numerical simulation of 3D printing extrusion processes can provide valuable information on the flow patterns which would be of huge importance, specially during the design stage [1]. While viscous fluids strain uniformly when a stress is applied, non-Newtonian shear-dependent fluids strain as a function of local shear rate, which is a characteristic of the fluid. The modeling and simulation of this kind of processing operations appears as a fundamental tool, which leads to a better understanding of how the rheological properties of printable biomaterials affect their processability, and reducing the time and costs related to the processes and the final products. The development of accurate numerical tools for the simulation of printable biomaterial multiphase flows is vital from both fundamental and practical points of view. Different approaches are used in literature to develop numerical tools to solve non-Newtonian multiphase flow problems. Among the various numerical methods available, finite-volume methods are reliable, flexible, fast and widely available tools, available in common simulation packages. Historically, the main challenges to be faced in the modeling of extrusion processes by means of finite-volume based solvers consist of: (1) the correct modeling of the non-Newtonian behavior apparent in many of the printable biomaterials; (2) the correct representation of the interface that divides the extruded fluid and the surrounding gas.

Regarding the representation of the interface, the Front-Tracking (Marker-and-Cell), Level-Set and Volume-of-Fluid (VoF) methods are known as the most widely used approaches in literature. The advantages and disadvantages of these methods in different applications have already been analyzed in the simulation of high-viscous Newtonian and non-Newtonian flows. In VoF methods [2], the advected scalar field function represents the volume fraction of one of the phases, varying from 0 to 1 in interface, and having the value of 0 or 1 in non-interface cells. Using this approach, Bonito et al. [3] assessed the appearance of buckling in 2D and 3D Jets. A disadvantage of the VOF method is its difficulty in computing accurate geometrical properties (interface normal and curvature) from the volume fraction function as it presents a step discontinuity. Alternatively, in the Level-Set Method (LSM) [4] the interface is identified by the zero contour of a signed level-set function, advected at every time step. Employing this approach, Ville et al. [5] carried out simulations of fluid extrusion for square and rectangular inlets. The major defect of LSM is due to the discrete solution of transport equations which leads to numerical errors in conservation of mass of the fluid-phase. In the Marker-and Cell method the individual interfaces are represented by sets of connected marker points. This approach is particularly effective in implementing free-surface approximations, where the effect of the gas is neglected, but performs quite inefficient when complex interfacial break-up and coalescence occur. Tome et al. [6] proved the ability of their updated MAC method on capturing physical instabilities regarding the buckling of planar jets with high-viscous and non-Newtonian properties.

The fluid buckling phenomenon is a challenging case usually employed to test the capability of numerical models to effectively represent the behavior of high-viscous and non-Newtonian fluids. The case consists of simulating a jet extruded downwards, under the effect of gravity, into a cavity. After hitting the solid base of the box, oscillations may appear on the free-surface of the jet, leading to coiling and folding patterns. Parameters influencing the appearance of buckling processes are the aspect ratio of the cavity H/D (where H is the height of the cavity in the gravity direction, and D is the jet width), the Reynolds

number of the jet, *Re*, the jet inlet section (circular, squared, rectangular) and the rheology of the jet. The validation of the implementation of the numerical methods in the context of the extrusion process has been done in our previous work [1] where the coiling process of a low Reynolds jet inside a cavity was predicted correctly.

In this work, direct numerical simulation of the Navier-Stokes equations in the context of the two-phase flows is used where the approach presented by [7] is utilized to resolve the non-Newtonian rheologies. The set-up presented by [8] for liquid extrusion simulations at high Re numbers is employed to impose inlet and outlet boundary conditions. The rest of the paper is organized as follows: mathematical formulation are presented in Section 2, numerical methods are described in Section 3. The numerical set-up is presented in Section 5, followed by the numerical results and discussion. Finally, conclusion remarks are provided in Section 6.

2 Mathematical Formulations

The numerical framework employed in this work accounts for a finite-volume discretization of Navier-Stokes equations for mass and momentum conservation on collocated unstructured meshes, Volume-of-Fluid description of the interface and Generalized-Newtonian-Fluid (GNF) models to take into account the non-Newtonian rheologies. A Volume-of-Fluid interface capturing approach is used to evaluate the time-evolution of the moving interface. In this approach, as explained before, the interface is captured implicitly using a scalar field $\alpha(\mathbf{x},t)$, representing the volume fraction of a phase inside each cell of the discretized domain at a given time:

$$\alpha(\mathbf{x},t) = \begin{cases} 1 & \text{cell is filled with associated phase} \\ 0 & \text{otherwise} \end{cases}$$

In this formulation, cells with $0 < \alpha(\mathbf{x},t) < 1$ are known as interface cells. For a given velocity field extracted from the Navier-Stokes equations, the time evolution of the interface is resolved using an advection equation as following:

$$\frac{\partial \alpha(\mathbf{x},t)}{\partial t} + \nabla \cdot (\alpha(\mathbf{x},t)\mathbf{u}) = 0. \tag{1}$$

A piecewise linear interface calculation (PLIC) method [9] is used to geometrically reconstruct the interface as planes with an arbitrary orientation in each interface cell. In this method, regardless of the grid cell type, i.e. structured or unstructured, the interface in each cell is defined as:

$$\mathbf{x} \cdot \mathbf{n} - d = 0 \tag{2}$$

where $\mathbf{n}$ is the unit-normal vector pointing outward with respect to the phase $\alpha(\mathbf{x},t)$, $\mathbf{x}$ is the position vector of a point on the interface and d is the signed distance from the origin to the plane. In this work, a point-cloud approach is used to evaluate the normal vectors of the interface cells [9].

The velocity scalar field, $\mathbf{u}(\mathbf{x},t)$, needed for the advection of the interface, is derived from the resolution of Navier-Stokes equations taking into account the incompressibility and variable properties limit (density, viscosity). In a domain occupied by two incompressible and immiscible fluids separated by an

interface, the velocity and pressure fields are governed by the following equations:

$$\frac{\partial}{\partial t}(\rho\mathbf{u}) + \nabla\cdot(\rho\mathbf{u}\mathbf{u}) = -\nabla p + \nabla\cdot\tau + \rho\mathbf{g} + \sigma\kappa\mathbf{n}\delta_\Gamma \quad (3)$$

$$\nabla\cdot\mathbf{u} = 0 \quad (4)$$

With the stress tensor evaluated as:

$$\tau = \mu(\dot{\gamma})\left(\nabla\mathbf{u} + (\nabla\mathbf{u})^T\right) \quad (5)$$

In this formulation, the apparent viscosity μ could be described as a function of shear-rate tensor $\dot{\gamma}$ in the context of Generalized Newtonian Fluid (GNF) formulation. A continuum surface force (CSF) approach [10] is used to transform the surface tension force into a volume force. The density and viscosity can be defined as scalar-fields inside the whole domain as follows:

$$\zeta = \zeta_1 H + \zeta_2(1-H) \quad (6)$$

where $\zeta \in \{\rho,\mu,\}$ and H is the Heaviside step function which takes the value one in dispersed phase and zero elsewhere.

3 Numerical Method

The numerical methods are implemented in an in-house parallel c++/MPI code called TermoFluids [11]. Validations and verifications of the numerical methods used in this work have been reported in [12, 13, 8, 14, 7, 18, 15, 16]. The Finite-volume (FV) approach is used to discretize the Navier-Stokes and VOF equations on a collocated grid, so all the computed variables are stored at cell centroids.

The algorithm employed to solve the governing equations described in Section 2 at each time-step can be described as follows:

1. Physical properties, interface geometric properties and velocity fields are initialized (only first iteration).
2. Allowable time step is calculated. The value of Δt is limited by CFL conditions on convective term and also by explicit treatment of surface tension as used by [14]. To decrease the computational costs, the maximum value of the CFL coefficient which leads to a stable simulation is used.
3. Using the evaluated normal vectors at the interface cells, the value of the d parameter in Equation 2 is calculated using the Brent's root-finding algorithm [17], thus, locating the interface planes of PLIC method at each interface cell.
4. In the context of finite-volume methods, the application of the divergence theorem and the spatial discretization of this equation over a cell with volume ∂v and face set F with area vectors of $d\mathbf{A}_f$ results to:

$$\int_{\partial v}\frac{\partial\alpha(\mathbf{x},t)}{\partial t} + \sum_{f_i\in F}(\alpha(\mathbf{x},t)\mathbf{u})_f\cdot d\mathbf{A}_{f_i} = 0 \quad (7)$$

   where the first term deals with the temporal evolution of the interface and the second term evaluates the total volumetric flux of the phase represented by volume-fraction function $\alpha(\mathbf{x},t)$ across the

faces of the associated grid cell in a timestep based on the selected temporal scheme. A geometrical approach as presented by Jofre et al. [12] is used to evaluate the second term by employing the geometrically reconstructed interface calculated based on volume fraction values at interface cells. In the classical formulation, the curvature is calculated as divergence of the gradient of color-function: $\kappa = \nabla \cdot (\nabla\alpha(\mathbf{x},t)/|\nabla\alpha(\mathbf{x},t)|)$. However, given the fact that the color-function in VOF is discontinuous by definition, applying derivative type operations to this discontinuous function leads to numerical errors. To circumvent this issue, a sign distance function (ψ) representing the minimum distance of each cell's center from the PLIC interface is evaluated in a neighbouring area of the interface. The curvature is then calculated using this continuous auxiliary distance-function as: $\kappa = \nabla \cdot (\nabla\psi/|\nabla\psi|)$ [9].

5. Density and viscosity in the domain and geometrical properties at the interface (curvature and interface normal) are updated from the advected color-function $\alpha(\mathbf{x},t)$ as described in Equation 6.

6. A semi-implicit fractional step projection method is used to solve the velocity-pressure coupling. In high-viscosity/non-Newtonian fluids, the varying value of viscosity can increase dramatically and lead to excessively small time-steps of the simulation and thus resulting in huge computational costs. To circumvent this issue, the diffusion term in equation 3 is treated implicitly. A second-order Adam-Bashforth scheme is used on convective, gravity, and surface tension terms. The proposed discretization for the predictor step was already presented and employed by the authors in [7, 13].

7. A correction to the predicted velocity applies as below:

$$\frac{\rho\mathbf{u}^{n+1} - \rho\mathbf{u}^{*}}{\Delta t} = -\nabla_h p^{n+1} \tag{8}$$

8. Poisson equation reads as follows and is solved using a preconditioned conjugated gradient method:

$$\nabla_h \cdot \left(\frac{1}{\rho}\nabla_h(p^{n+1})\right) = \frac{1}{\Delta t}\nabla_h \cdot (\mathbf{u}^{*}) \tag{9}$$

9. The velocity $\mathbf{u}^{n+1}$ is corrected by the updated pressure as:

$$\mathbf{u}^{n+1} \quad = \quad \mathbf{u}^{*} - \frac{\Delta t}{\rho}\nabla_h(p^{n+1}) \tag{10}$$

4 Extraction of the rheological properties

0.6 g of 30 wt. % pluronic F127 (BASF pharmaceutics, Germany) hydrogel were loaded with 1.4 g β-tricalcium phosphate fine powder (3-4 μm particle size that was sintered and milled in the laboratory) in a dual asymmetric centrifugal mixer (DAC 150, Speedmixer, USA), in order to create a printable ceramic slurry. The rheological characterisation was carried out in a rotational rheometer (Discovery HR-2, TA Instrument) after 5 min of the ceramic paste preparation, using a rough parallel plate geometry with a 20 mm diameter, a 0.5 mm gap (higher than 10 times the particles size) and solvent trap. The test consisted in an amplitude sweep from 0.01 to 2000 % strain with a frequency of 1Hz, a temperature of 23 ºC and 50 points per decade.

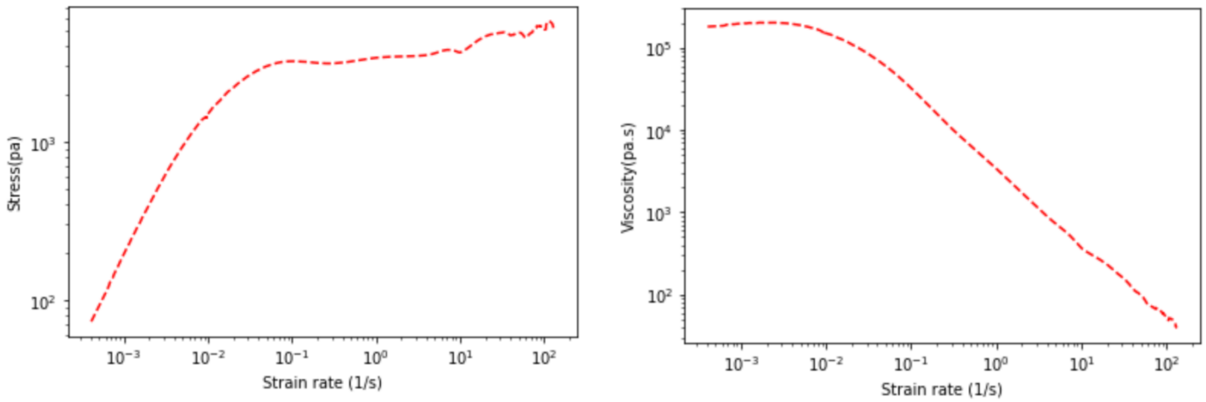

Figure 1: Stress vs. Strain-rate (left), Viscosity vs. Strain-rate (right) of the experimental data.

To be able to use these data in the numerical solvers, it is important to find the mathematical formulation describing the rheological properties of the fluid. First step is to identify the type of non-Newtonian fluid (shear-thinning, shear-thickening, viscoelastic, etc.) and after that the task is to extract the related mathematical formulation and its associated parameters, e.g. power factor, solvent viscosity, polymer viscosity, relaxation time etc.

The experimental data contains stress values ranged between 73.3426 to 5813.77 Pa. Figure 1 illustrates the stress (pa) vs. strain-rate (1/s) and viscosity (Pa.s) vs strain-rate (1/s) plots. It can be seen that the viscosity vs. strain-rate graph exhibits behaviour similar to shear-thinning material. Power-law (Eq. 11), Carreau-Yasuda (Eq. 12), and Cross (Eq. 13) models are amongst the most famous equations for this type of material:

$$\mu = m|\dot{\gamma}|^n \tag{11}$$

$$\mu = \mu_\infty + (\mu_0 - \mu_\infty)\left(1 + (m|\dot{\gamma}|)^a\right)^{\frac{n-1}{a}} \tag{12}$$

$$\mu = \mu_\infty + \frac{\mu_0 - \mu_\infty}{1 + (m|\dot{\gamma}|)^n} \tag{13}$$

An effort was done to fit these formulas to the experimental data. Non-linear least-squares method was used to minimize the cost function representing the differences of the experimental data and the given equation. The open-source machine learning library scikit-learn was used for this task. The best fit was achieved by cross model rheological type, as depicted in figure 2. The mathematical formulation for this model would be as:

$$\mu = 1 + \frac{205273}{1 + (41.38|\dot{\gamma}|)^{1.25}} \tag{14}$$

5 Numerical experiments and discussion

The test case analyzed in the current work consist of a low Reynolds number extrusion of liquid l into a rectangular box filled by quiescent gas g. The numerical set-up, depicted in Fig. 3, consists of a rectangular box, where a heavier fluid is extruded from a circular shaped inlet of dimension D with

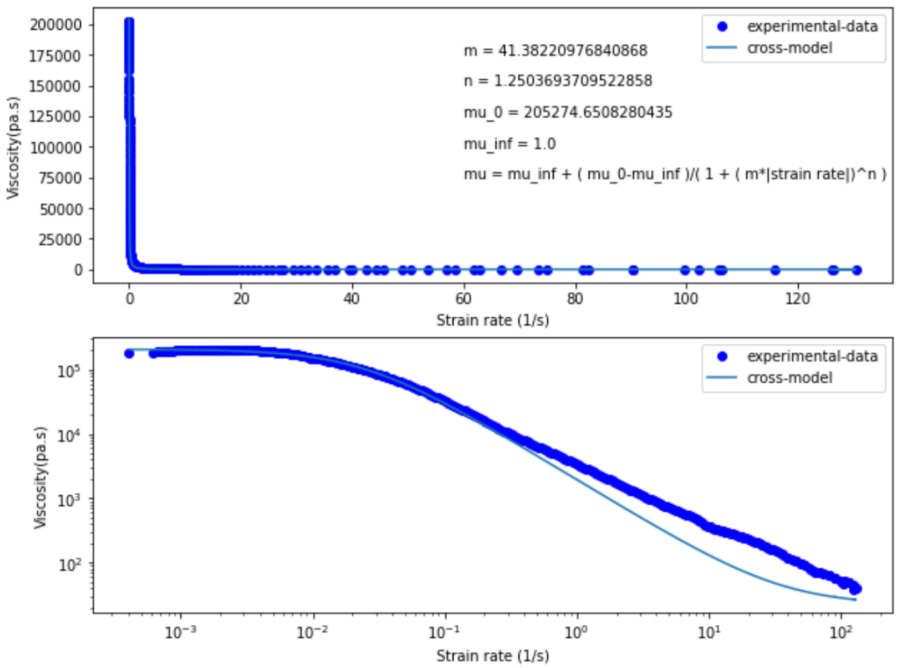

Figure 2: Extracted viscosity vs. strain-rate for cross model.

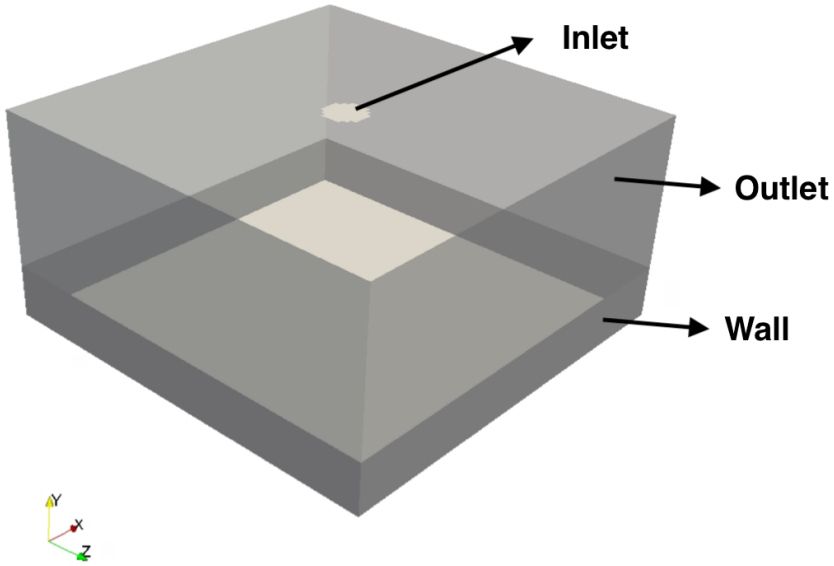

Figure 3: The geometry used for the simulation of the jet extrusion.

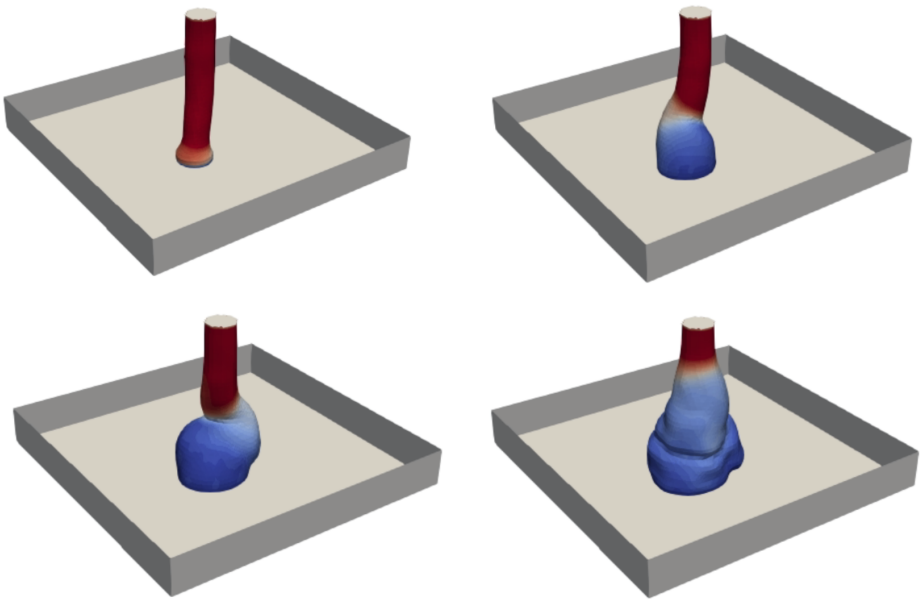

Figure 4: Time evolution of the printable biomaterial Jet in a domain with H/D=10

a constant inlet velocity, u_l. The rectangular box has height of H equal to $10D$. An outlet pressure is imposed at the outlet boundaries, allowing the gas to go out of the domain as the liquid jet is being extruded. The domain is discretized into (80, 40, 80) cubic cells in (x, y, z) directions, hence, a structured mesh is employed.

Figure 4 illustrates the evolution of the extruded jet. Regardless of the time scale of the problem, we are here exclusively interested in analyzing the evolution of the free surface during the discharge process. The extruded liquid starts to fold immediately once it reaches the cavity floor. Hence, toroidal oscillations appear and the jet starts to coil into itself with a regular frequency. Due to the high viscosity, however, no break-up process of the free surface is visible, which will tend to fill the vessel on a regular basis. Figure 5 illustrates the time evolution of the extruded jet in which the bottom plane is moving with the velocity of u_l. The extruded liquid illustrates non-uniform oscillations before and after impacting the bottom wall.

6 Conclusion

This paper presents the results obtained in the simulation of non-Newtonian printable ceramic ink characterized by high viscosity, applying a low printing speed. The numerical method presented incorporates the finite-volume based/direct numerical simulation of the Navier-Stokes equations for a multiphase flow consisting of a fluid and a gas. The transport of the interface is carried out through a geometrical VoF method. The numerical methodology used in this work has been rigorously validated and verified in previous works, especially in the context of numerical simulation of Newtonian/non-Newtonian fluids extrusion process, used in 3D printing processes. The rheological formulation is extracted by fitting a Cross type model into the experimental data. The numerical methodology presented proves to be stable

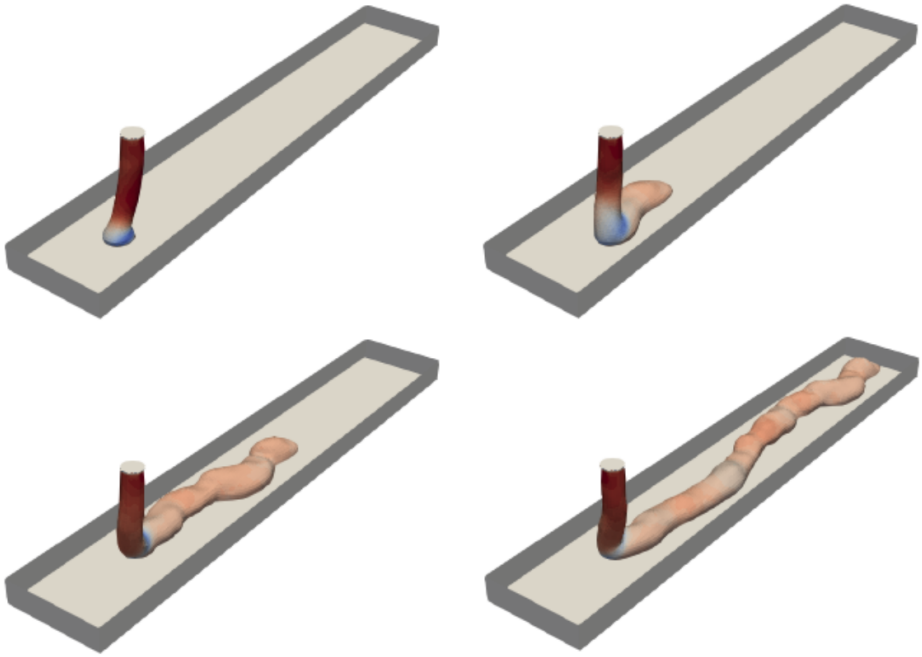

Figure 5: Time evolution of the printable biomaterials Jet in a domain with H/D=10, where the bottom wall is moving with the u_l velocity.

and conservative. Two test cases of extruding printable biomaterials into a cavity are solved, where in one case, the bottom wall is fixed and in the other one the bottom wall is moving with a fix velocity, to simulate the relative displacement of the printing nozzle and the substrate. As the next step, the results of these simulations will be compared with their experimental countrparts.

Acknowledgments

This work was developed in the context of a research project (BASE3D 001-P-001646) co-financed by the European Union Regional Development Fund within the framework of the ERDF Operational Program of Catalonia 2014-2020 with a grant of 50% of total cost eligible.

REFERENCES

[1] A. Amani, E. Schillaci, D. Kizildag, C.D.P Segarra. *Numerical Analysis of viscoelastic fluid injection process*. 14th World Congress on Computational Mechanics (WCCM), ECCOMAS Congress 2020.

[2] Hirt, Cyril W and Nichols, Billy D. *Volume of fluid (VOF) method for the dynamics of free boundaries*. Journal of Computational Physics, 1981, 201–225.

[3] Bonito, Andrea and Picasso, Marco and Laso, Manuel. *Numerical simulation of 3D viscoelastic flows with free surfaces*. Journal of Computational Physics, 2006, 691–716.

[4] Osher, Stanley and Sethian, James A. *Fronts propagating with curvature-dependent speed: algorithms based on Hamilton-Jacobi formulations*. Journal of Computational Physics, 1988, 12–49.

[5] Ville, Laurence and Silva, Luisa and Coupez, Thierry. *Convected level set method for the numerical simulation of fluid buckling*. International Journal for Numerical Methods in Fluids, 2011, 324–344.

[6] Tome, Murilo F and McKee, Sean. *Numerical simulation of viscous flow: Buckling of planar jets*. International Journal for Numerical Methods in Fluids, 1999, 705–718.

[7] A. Amani, N. Balcázar, A. Naseri and J. Rigola. *A numerical approach for non-Newtonian two-phase flows using a conservative level-set method*. Chemical Engineering Journal, 385 (Apr. 2020), p. 123896.

[8] E. Schillaci, O. Antepara, N. Balcázar, J. Rigola, A. Oliva. *A numerical study of liquid atomization regimes by means of conservative level-set simulations*. Computers & Fluids, 2019, 137–149.

[9] Amani, A, Muela, J, Schillaci, E, Castro, J. *On estimating the interface normal and curvature in piecewise linear interface calculation-volume of fluid approach for three-dimensional arbitrary meshes*. AIChE Journal, 2022.

[10] Brackbill, J U and Kothe, Douglas B and Zemach. *A continuum method for modeling surface tension*. Journal of Computational Physics, 1992, 335–354.

[11] *Termo Fluids S.L.*. http://www.termofluids.com.

[12] J. Lluís, O. Lehmkuhl, J. Castro, A. Oliva. *A 3-D Volume-of-Fluid advection method based on cell-vertex velocities for unstructured meshes*. Computers and Fluids, 2014, 14–29.

[13] A. Amani, N. Balcázar, J. Castro, A. Oliva. *Numerical study of droplet deformation in shear flow using a conservative level-set method*. Chemical Engineering Science, 2019, 153–171.

[14] A. Amani, N. Balcázar, E. Gutiérrez, A. Oliva. *Numerical study of binary droplets collision in the main collision regimes*. Chemical Engineering Journal, 2019, 477–498.

[15] A. Amani, N. Balcázar, A. Naseri, A. Oliva. *A Study on Binary Collision of GNF Droplets Using a Conservative Level-Set Method*. 7th European Conference on Computational Fluid Dynamics (ECFD 7), Glasgow, UK, 2018.

[16] A. Amani, N. Balcázar, E. Gutiérrez, A. Oliva. *DNS of un-equal size droplets collision using a moving-mesh/level-set method*. ERCOFTAC workshop direct and large eddy simulation 12 (DLES 12), Madrid, Spain, 2019.

[17] Ermentrout, G.B., *Numerical recipes in C*. 1989.

[18] Gutiérrez, E and Favre, F and Balcázar, N and Amani, A and Rigola, J. *Numerical approach to study bubbles and drops evolving through complex geometries by using a level set-Moving mesh-Immersed boundary method*. Chemical Engineering Journal, 2018, 662–682.